STEM CELLS TRANSLATIONAL MEDICINE®

EMBRYONIC STEM CELLS/INDUCED PLURIPOTENT STEM (iPS) CELLS

Expansive Generation of Functional Airway Epithelium From Human Embryonic Stem Cells

BRENDAN A.S. MCINTYRE,[a] CANTAS ALEV,[b] RAMI MECHAEL,[a,c] KYLE R. SALCI,[a,c] JUNG BOK LEE,[a] ALINE FIEBIG-COMYN,[a] BORHANE GUEZGUEZ,[a] YUPING WU,[b] GUOJUN SHENG,[b] MICKIE BHATIA[a,c]

Key Words. Acute lung injury • Air-liquid interface • Differentiation • Human embryonic stem cells

[a]McMaster Stem Cell and Cancer Research Institute, Michael G. DeGroote School of Medicine, McMaster University, Hamilton, Ontario, Canada; [b]Laboratory for Early Embryogenesis, RIKEN Center for Developmental Biology (CDB), Kobe, Japan; [c]Department of Biochemistry and Biomedical Sciences, McMaster University, Hamilton, Ontario, Canada

Correspondence: Mickie Bhatia, Ph.D., Stem Cell and Cancer Research Institute, McMaster University, Faculty of Health Sciences, 1280 Main Street West, MDCL 5029, Hamilton, Ontario L8S 4K1, Canada. Telephone: 905-525-9140, ext. 28687; E-Mail: mbhatia@mcmaster.ca

Received June 26, 2013; accepted for publication September 6, 2013; first published online in SCTM *EXPRESS* December 3, 2013.

1066-5099/2013/$20.00/0

http://dx.doi.org/10.5966/sctm.2013-0119

ABSTRACT

Production of human embryonic stem cell (hESC)-derived lung progenitors has broad applicability for drug screening and cell therapy; however, this is complicated by limitations in demarcating phenotypic changes with functional validation of airway cell types. In this paper, we reveal the potential of hESCs to produce multipotent lung progenitors using a combined growth factor and physical culture approach, guided by the use of novel markers LIFRα and NRP1. Lung specification of hESCs was achieved by priming differentiation via matrix-specific support, followed by air-liquid interface to allow generation of lung progenitors capable of in vitro maturation into airway epithelial cell types, resulting in functional characteristics such as secretion of pulmonary surfactant, ciliation, polarization, and acquisition of innate immune activity. This approach provided a robust expansion of lung progenitors, allowing in vivo assessment, which demonstrated that only fully differentiated hESC-derived airway cells were retained in the distal airway, where they aided in physiological recovery in immunocompromised mice receiving airway injury. Our study provides a basis for translational applications of hESCs for lung diseases. STEM CELLS TRANSLATIONAL MEDICINE *2014;3:7–17*

INTRODUCTION

Human endodermal specification into functional pancreatic [1], hepatic [2], thymic [3], or lung [4] cell types from human embryonic stem cells (hESCs) has proven complex [5]. These studies describe multistep processes and require the culture of hESC-derived cells over extensive periods to permit generation of cells that acquire marker expression based on mouse embryology, associated with putative lineage-specific progenitors [1–3]. Signaling mechanisms involved in mouse endoderm development have been exploited using hESCs to generate putative lung progenitors [4, 6, 7], although evidence for subsequent maturation and functional tissue integration has yet to be demonstrated. Accordingly, the translational impact of these studies using hESC differentiation schemas [4, 8–10] remains unclear [5, 11]. In addition to the heterogeneous nature of differentiation from hESCs, the impact of these studies will ultimately depend on functional capacity and measurement of the fully mature cell types derived. To date, the only successfully derived endodermal cell type used for experimental cell therapy in animal models has been pancreatic cells [12, 13]. Noteworthy is that these experiments were most successful not with pure sorted populations but rather with heterogeneous mixtures of pancreatic and other cell types [12, 13]. For airway epithelia, functional long-term human engraftment studies in xenograft models have yet to be performed. In this study, we describe a novel approach to obtaining hESC-derived lung epithelial progenitor cells that have functional properties. Because of the expansive nature of this protocol, we have been able to test and validate the functionality of these hESC-derived airway cells in vivo using a mouse xenograft transplantation model following acid-induced acute lung injury.

MATERIALS AND METHODS

Cell Culture

All experiments were performed using hESC lines CA2 [14] and H9 [14] grown on Matrigel (BD Biosciences, San Diego, CA, http://www.bdbiosciences.com) and passed 1:2 by dissociation with collagenase IV for $\leq$5 minutes. Where explicitly indicated, certain experiments also included a dermal derived induced pluripotent stem (iPS) cell line (iPS1.2 [15]), and data from these three lines were averaged. Cells were cultured in atmospheric oxygen and maintained in either mTeSR1 (StemCell Technologies, Vancouver, BC, Canada, http://www.stemcell.com) or mouse embryonic fibroblast-conditioned medium (MEF-CM) supplemented with 8 ng/ml basic fibroblast growth factor (bFGF), with daily media changes. Daily morphological evaluation of cells was made by stereo binocular light microscopy

(Nikon, Tokyo, Japan, http://www.nikon.com) with routine monitoring of pluripotency marker expression (stage-specific embryonic antigen 3, TRA-1-60) by flow cytometry. Control primary human small airway epithelial cells were propagated in bronchial epithelial growth media (BEGM; Lonza, Walkersville, MD, http://www.lonza.com) and switched to Clonetics B-ALI air-liquid interface (ALI) medium for ALI culture (Lonza). Experiments represent averaged results from these two hESC lines unless stated otherwise.

hESC Priming and Differentiation in ALI

Optimal conditions for airway cell differentiation were as follows: HESCs, which were grown for more than five passages in mTeSR1 on 1:15 Matrigel to KnockOut (KO) Dulbecco's modified Eagle's medium (DMEM), were stimulated to form definitive endoderm (DE) by addition of 100 ng/ml activin A (AA) to mTeSR1 for 5 days with daily feeding. Cells were passaged with collagenase IV, triturated 10 times, and pipetted through a 35-μm strainer cap test tube (BD Biosciences). Noteworthy is that spontaneous neural outgrowths observed in mTeSR1 were removed by manual scraping. Cells were counted using an automated cell counter (Countess; Invitrogen, Carlsbad, CA, http://www.invitrogen.com) and viability assessed by trypan blue exclusion. Then, 5–10 $\times$ 10^3 live cells were plated on Matrigel-coated polyester membrane inserts with 0.5-μm pores adapted for 24-well tissue culture plates (Costar 3470; Corning Costar, Acton, MA, http://www.corning.com/lifesciences). Subsequently, cells had 2–3 days of liquid-liquid culture in mTeSR1, followed by maintenance for 2–3 days in mTeSR1 or differentiation media [9] (80% KO-DMEM, 20% KO serum replacement, 2 mM L-glutamine, and 1% nonessential amino acids [Invitrogen], termed "bFGF-free differentiation media"), for a total of 4–6 days in liquid-liquid culture (until a monolayer was formed). An "air-lift" procedure was then performed in which liquid was removed from the apical or upper surface and cells fed only from the basolateral or lower side, with media changes every other day. This procedure is referred to as ALI culture. After 5 days of ALI, cells were split using TrypLE (Invitrogen), triturated 30–40 times, and pipetted through a 35-μm strainer cap test tube and doubled by plating on two new inserts coated in Matrigel. Liquid-liquid culture was then repeated for 3–6 days (until a monolayer was formed), followed by ALI for a minimum of 30 days and a maximum of 50 days, with media changes occurring (basally only) every other day. Continued culture in bFGF-free differentiation media results in functional airway cell differentiation, as described. For lipopolysaccharide (LPS) stimulation, recombinant LPS (Sigma-Aldrich, St. Louis, MO, http://www.sigmaaldrich.com) was added to cultures at 1-μg/ml concentrations in 20 μl apically and 500 μl basally in media for 5 hours.

Embryonic Array Analysis

Fertilized chicken eggs were incubated at 38.5°C for 5 hours. The area pellucida (AP) region of the embryos, containing both epiblast and hypoblast, was cut out in Pannett-Compton buffer. In half of the dissected AP samples, the hypoblast was further removed and the remaining pure epiblast tissues were pooled and used for RNA isolation. Two independent sets of total RNA from six AP samples and six epiblast-only samples were isolated with the RNeasy Micro kit (Qiagen, Hilden, Germany, http://www.qiagen.com)., Using two-cycle cRNA labeling protocols (Affymetrix, Santa Clara, CA, http://www.affymetrix.com), 100 ng of quality-checked total RNA were used per array. High-density *Gallus gallus* arrays (GeneChip Chicken Genome Array; Affymetrix) were hybridized according to the Expression Analysis Technical Manual (Affymetrix), and analysis of resulting expression levels was performed as reported [16]. Probe sets with a ratio $>$1.5 between maximum and minimum mean expression levels among two sample sets (AP vs. epiblast) were examined for genes coding for cell-surface receptors and membrane-associated proteins.

Flow Cytometry and Sorting

Flow cytometry was carried out using preconjugated primary antibodies at the indicated concentrations in 3% fetal calf serum in phosphate buffered saline (FCS/PBS) with an LSR II for analysis and FACSAria for sorting (BD Biosciences). All antibodies and reagents were purchased from BD Biosciences unless stated otherwise: CXCR4-PE (1:50), CXCR4-APC (1:100), LIFRα-PE (1:50; R&D Systems Inc., Minneapolis, MN, http://www.rndsystems.com), NRP1-APC (1:100, R&D Systems), TRA-1-60-Alexa-488 (1:200), SSEA-3-PE (1:100). All results are based on live cell staining by gating on 7-aminoactinomycin D-negative populations (1:50). All analysis and flow graphing was done in FlowJo (Tree Star, Ashland, OR, http://www.treestar.com).

Tissue Harvesting and Flow Cytometry From Transplanted Mouse Lungs

Two lobes of right lung were harvested from euthanized mice, minced using scalpels, and placed in 3% FCS/PBS (wash buffer). Tissue was then digested overnight with 0.4 U/ml collagenase B at 4°C. Tissues were then dissociated by trituration, washed, and red blood cells lysed in 1$\times$ ammonium chloride red blood cell lysis buffer for 5 minutes at 4°C (StemCell Technologies), washed again, and dissociated with phosphate buffered saline-based single-cell dissociation solution (Invitrogen) for 15 minutes at 37°C. Cells were then washed and resuspended in 3% FCS/PBS. The following antibodies were used: mouse-specific CD11b-PE-Cy7 was used at 1:500 (BD Biosciences); unconjugated anti-human acetylated tubulin (Sigma-Aldrich) was used at 1:1,000, followed by secondary staining with anti-mouse Alexa-647 (Life Technologies) used at 1:1,000 with two washes with 3% FCS/PBS following antibody staining. Flow cytometry was run and analyzed, as indicated previously.

Whole-Mount RNA In Situ Hybridization

In situ hybridization of chicken embryos (stage HH4 [17]) was performed as described previously [18, 19]. Sectioning of paraffin-embedded embryos was performed using a Microm HM325 microtome (10 μm). Whole-mount images were taken with an SZX12 microscope and images of sections with a BX51 microscope, both mounted to a DP70 camera (Olympus, Tokyo, Japan, http://www.olympus-global.com). In situ hybridization probes of genes used in this work correspond to the following National Center for Biotechnology Information sequences: *CXCR4* (nt 706–1163 of AF294794), *GATA6* (nt 561–1032 of NM_205420), *LIFR*α (nt 3271–3795 of NM_204575), *NRP1* (nt 1481–2104 of NM_204782).

RNA Extraction and Quantitative Polymerase Chain Reaction

RNA was extracted from cells using the "All-in-One" purification kit according to the manufacturer's protocol (Norgen Biotek Corp.,

Thorold, Ontario, Canada, http://norgenbiotek.com). Quantitative polymerase chain reaction (qPCR) was performed on a CFX-96 machine running CFX Manager software (Bio-Rad, Hercules, CA, http://www.bio-rad.com). The GoTaq qPCR master mix (Promega, Madison, WI, http://www.promega.com) was used for all reactions, with fluorescence read in the SYBR green channel. Data were analyzed using the comparative C_t method ($2^{-\Delta\Delta Ct}$) with 18S ribosomal RNA, glyceraldehyde-3-phosphate dehydrogenase, and TATA-binding protein serving as control genes. Student's *t* test was used to determine statistical significance between groups. All qPCR runs included β-glucuronidase as a metric for C_t background cutoff.

Histology and Immunohistochemistry

Assistance for histological analysis was provided by the core histology laboratory of the department of pathology and molecular medicine at McMaster University (Hamilton, Ontario, Canada). Briefly, ALI cassette inserts were removed and placed into 10% formalin overnight at 4°C. The next day, cassettes were washed with 50% ethanol for 10 minutes, placed into 70% ethanol, and embedded in paraffin wax. Sections were then cut on a microtome to a thickness of 10 μm. Sections were then rehydrated and stained in periodic acid-Schiff-Alcian blue or hematoxylin-eosin following established protocols and evaluated histologically.

Immunofluorescent Staining of Paraffin-Embedded Tissues and Fixed Cells

Immunofluorescent staining was performed on paraffin-embedded tissues that were deparaffinized and blocked in 5% FCS/PBS or on tissue culture plates from cells fixed with 100% methanol for 15 minutes at 4°C. Primary antibodies diluted in 5% FCS/PBS were used at the following concentrations: rabbit anti-pro-SP-C at 1:250 (AB3786; Millipore, Billerica, MA, http://www.millipore.com) and mouse anti-acetylated tubulin at 1:1,000 (T6793; Sigma-Aldrich), goat anti-FoxA2 at 1:200 (SC-9187; Santa Cruz Biotechnology Inc., Santa Cruz, CA, http://www.scbt.com), rabbit anti-NKX2.1 at 1:200 (SC-13040; Santa Cruz Biotechnology), mouse anti-NKX2.1 at 1:200 (SC-53136; Santa Cruz Biotechnology), and mouse anti-OCT4 at 1:200 (SC-5279; Santa Cruz Biotechnology). Secondary antibodies, used at 1:500, donkey anti-rabbit DL488 (green channel), donkey anti-mouse Alexa Fluor 647 (far red), and donkey anti-goat DL488 or DL647 (depending on the combination used). All antibodies were incubated overnight at 4°C in a humidified chamber. Slides and plates were washed 3 times in PBS-0.05% Tween-20 before primary and secondary antibody incubation. Hard-set 4′,6-diamidino-2-phenylindole (DAPI) mounting media (Vector Laboratories, Burlingame, CA, http://www.vectorlabs.com) was directly applied to PBS rinsed slides with coverslips or at 1:1,000 in PBS for cells stained in vitro on tissue culture plates. Confocal imaging was performed using an inverted spinning disk confocal microscope (Olympus), where indicated. Regular immunofluorescent staining was taken using an inverted fluorescent microscope (Olympus). Images from both systems were captured with Metamorph software (Molecular Devices LLC, Sunnyvale, CA, http://www.moleculardevices.com/) and overlays with phase and DAPI made using the open source ImageJ software suite. For ZO-1 (TJP1) antibody (HPA001636, used at 1:200; Sigma-Aldrich), staining was performed "en face," with fixation in acetone, with subsequent blocking and washing steps performed as described.

Fluorescent DNA In Situ Hybridization

Fluorescein isothiocyanate-conjugated human Alu Repeat DNA probes (BioGenex, Fremont, CA, http://www.biogenex.com/) were used as described previously [20]. Briefly, slides were deparaffinized as described and washed in 2× saline-sodium citrate (SSC) buffer. The probe was warmed and mounted with a coverslip onto slides at 37°C for 10 minute. Slides were placed on a hot plate at 75°C for 90 minutes and then dipped in a 72°C water bath to remove coverslips and washed in 0.4× SSC at 72°C and twice in 2× SSC 0.05% Tween-20 at room temperature for 5 minutes. Slides were then coverslipped with DAPI and imaged as described previously.

Transepithelial Electrical Resistance

Transepithelial electrical resistance was measured under a constant current of 10 μA using an epithelial volt-ohm meter (EVOM^2; World Precision Instruments, Sarasota, FL, http://www.wpiinc.com). Electrodes were placed both apically and basally with KO-DMEM added apically to cover the electrode.

Enzyme-Linked Immunosorbent Assay

Surfactant protein D (SP-D) levels were measured in apical secretions of cells grown in ALI or control liquid cultures using the Quantikine Human SP-D Immunoassay (R&D Systems) according to the manufacturer's protocols. Briefly, the apical surface, which contains a viscous layer after ALI, was briefly rinsed with 50–100 μl of KO-DMEM and collected and stored at −80°C until use. SP-D protein concentrations were then calculated based on a standard curve generated from human recombinant SP-D. Absorbance was measured at 450 nm and corrected by subtracting background at 540 nm on a BMG FluoStar Omega plate reader (Imgen Technologies, Alexandria, VA, http://www.imgen.com/).

Acid-Induced Lung Injury Model

An in vivo murine model of acute lung injury was used [21], with all mice bred and maintained in the Stem Cell and Cancer Research Institute animal barrier facility at McMaster University. All animal procedures received the approval of the animal ethics board at McMaster University. Briefly, 30–50 μl of 0.1 M hydrochloric acid (HCl) and 0.3% PBS (pH 1.25) was instilled by the intratracheal route into anesthetized NOD.CB17-Prkdc^{scid}/J (NOD-SCID) mice (Jackson Laboratory, Bar Harbor, ME, http://www.jax.org). HCl administration was performed using a fiber optic mouse BioLite intubation kit (Braintree Scientific Inc., Braintree, MA, http://www.braintreesci.com/). After monitoring for breathing rate stability for 1 hour, saline vehicle or 0.5×10^5 to 2.5×10^5 cells (bFGF-free differentiated or mTeSR1 undifferentiated hESCs) or 2×10^6 15-μm blue-green fluorescent microspheres (Invitrogen) were administered intravenously via tail vein. Mice were harvested 24 hours after intravenous injection of beads and processed using an alternative protocol necessitated to preserve bead integrity [22]. Prior to administration, cells were labeled with 2 μl/ml CellTracker Vybrant CM-DiI, which has been chemically modified to resist formalin fixation and paraffin embedding, following the manufacturer's instructions (Invitrogen). The ability of the cells to retain fluorescent dye was first tested by replating labeled cells on Matrigel for $>$1 week and examining fluorescence intensity. At the indicated

time points, oxygen saturation (SpO_2) was recorded using a pulse oximeter on grouped animals on the same day to account for experimental variability (PhysioSuite; Kent Scientific Corporation, Torrington, CT, https://www.kentscientific.com/). Animals were sacrificed and weighed, and lungs were removed for histological processing at the indicated time points. For histological sections, lungs were processed as noted previously. CM-DiI was imaged in the CY3 channel and microspheres were imaged in the GFP channel, along with DAPI nuclear staining and phase contrast (bright field), using an inverted fluorescent microscope (Olympus). Images were captured with Metamorph software (Molecular Devices) and overlays, with phase and DAPI made using the open source ImageJ software suite.

Microchimerism Polymerase Chain Reaction

Presence of human genomic DNA (gDNA), chromosome 17 α-satellite, was evaluated in acid-injured lungs that received transplanted human cells and control uninjured lungs, according to previously published protocols [23, 24]. A standard curve of control human gDNA from 100 pg/μl to 1 pg/μl was included. Polymerase chain reaction products were run on a 1% agarose gel and imaged using an EpiChem3 BioImaging system and PC running Vision Works LS version 7.0.1 (UVP LLC, Upland CA, http://www.uvp.com/visionworks.html). Sample gDNA was purified using the DNeasy blood and tissue kit (Qiagen) and quantified on an ND-1000 spectrophotometer (NanoDrop, Wilmington, DE, http://www.nanodrop.com).

Statistical Analysis

Statistical testing was performed using GraphPad Prism version 5.0a by application of either ANOVA, for grouped flow cytometry kinetics, or Student's *t* test, for qPCR results (GraphPad Software, Inc., San Diego, CA, http://www.graphpad.com). A threshold *p* value of $<.05$ was used to determine statistical significance.

RESULTS

Novel Markers Reveal the Ability to Prime hESCs for Endodermal Lineage

Compared with ectoderm and mesoderm [25, 26], the endoderm has traditionally been a lineage with a very limited choice of cell surface markers to characterize differentiation events. Currently, CXCR4 is the only cell surface marker utilized to describe DE differentiation in mice [27] and humans [28], but it comprises a subset of extremely heterogeneous cell types [6, 7], making optimization of differentiation difficult to interpret [5, 11]. Using an established approach of embryonic microdissection that provides robust transcriptomic data of the gastrulating embryo [16], we performed an embryonic germ layer screen of avian embryos aimed at isolating novel endodermal cell surface markers. A total of five candidates encoding cell surface markers from this screen were prioritized and included independent identification of CXCR4 (Fig. 1A). Top candidates showed fold enrichment of *CXCR4* (6.9×), *NRP1* (4.3×), *GPC3* (4.2×), *LIFR*α (3.3×), *CD3e* (2.1×). In addition, TFs associated with endodermal differentiation [29] were also found to be upregulated with the following fold enrichment: *SOX17* (5.6×), *HNF4A* (5.4×) *GATA6* (4.0×), *FOXA2* (2.6×). The top candidates from the newly identified surface markers were then evaluated by in situ hybridization during avian embryonic development demonstrated here by their expression at developmental stage 4 (HH4) [17] and were compared with the known intracellular endodermal marker *GATA6* [29] (Fig. 1B).

Using these known and novel differentiation markers, we tested the hypothesis that initial hESC endodermal differentiation can be primed under specific culture conditions [30], given the prolonged culture conditions required for other endodermal lineages to develop from hESCs [1–3]. Under feeder-free conditions, we identified that hESCs grown on Matrigel in chemically defined media mTeSR1 [31] versus MEF-CM supplemented with bFGF allowed phenotypic conversion of hESCs to cells with enhanced expression of the endodermal protein marker CXCR4 after multiple passages (Fig. 1C). This also correlated to an increased expression of endodermal-specific transcription factors—*GATA6*, *FOXA2*, and *SOX17* (Fig. 1D, 1E)—required for DE formation and anterior foregut endoderm patterning [29, 32] and resulted in stable levels of CXCR4-positive hESCs. Consistent with enhanced endoderm marker expression of hESCs cultured in mTeSR1, NRP1 and LIFRα were also expressed at high levels that could be augmented along with CXCR4 in the presence of AA in serum-free mTeSR1 cultures (Fig. 1F).

These newly identified genes were also evaluated by qPCR comparisons from purified subsets of CXCR4-positive and CXCR4-negative hESCs, demonstrating higher expression in CXCR4-positive subsets (Fig. 1G). To provide a more direct evaluation, NRP1-positive and LIFRα-positive hESCs were purified and used to evaluate pluripotency (*OCT4*) and early endodermal transcription factor expression for *GATA6*, *FOXA2,* and *SOX17* (Fig. 1H). Endodermal marker expression was found to be enriched in LIFRα-positive and NRP1-positive hESC fractions compared with unfractionated hESCs (Fig. 1H), validating these novel cell surface markers in early endoderm potentiation of hESCs. Further qPCR characterization of the gene expression signature of hESCs sorted for CXCR4, LIFRα, or NRP1 early endodermal markers revealed additional enrichment of early mesodermal markers (*T*) but not ectodermal markers (*SOX2*, *NESTIN*) or neural crest markers (*NOTCH1*, *NOTCH2*) (supplemental online Fig. 1).

In Vitro Differentiation of Airway Epithelium Using bFGF-Free Dual ALI Culture

We next evaluated differentiation potential of hESCs with enhanced DE marker expression using subsequent ALI culture for further development toward lung epithelial progenitors, as illustrated in Figure 2A. The hESCs were primed by serial culture in feeder-free mTeSR1 media and treated with 100 ng/ml of AA for 5 days prior to transfer to transwell inserts coated with Matrigel. Subsequently, three scenarios were tested. Primed cells adapted to mTeSR1 were maintained in mTeSR1 growth media, placed in bFGF-free differentiation media [9], or assayed against initial starting conditions consisting of cells not adapted to mTeSR1 but maintained in MEF-CM throughout. The use of undefined commercial media BEGM and B-ALI (Lonza), reported in a recent directed differentiation protocol [10], was avoided because of xenogenic products (bovine pituitary extract) and undisclosed, proprietary additives (B-ALI inducer; Lonza). On formation of a monolayer of cells, media in the apical (upper) chamber of the transwell were removed and cultures were sustained from the basolateral side only (ALI culture). ALI culture with MEF-CM created large areas of pigmented cells clearly not associated with lung (supplemental online Fig. 2A). In contrast, ALI culture in bFGF-free differentiation media [9] was associated with

A

Avian Endodermal Embryonic Screen

Rank	Gene Title	Symbol
1	Chemokine Receptor-4 (CD304)	CXCR4
2	Neuropilin-1 (CD304)	NRP1
3	Glypican-3	GPC3
4	Leukemia Inhibitory Factor Receptor-α	LIFRα
5	CD3e (CD3-TCR complex)	CD3e

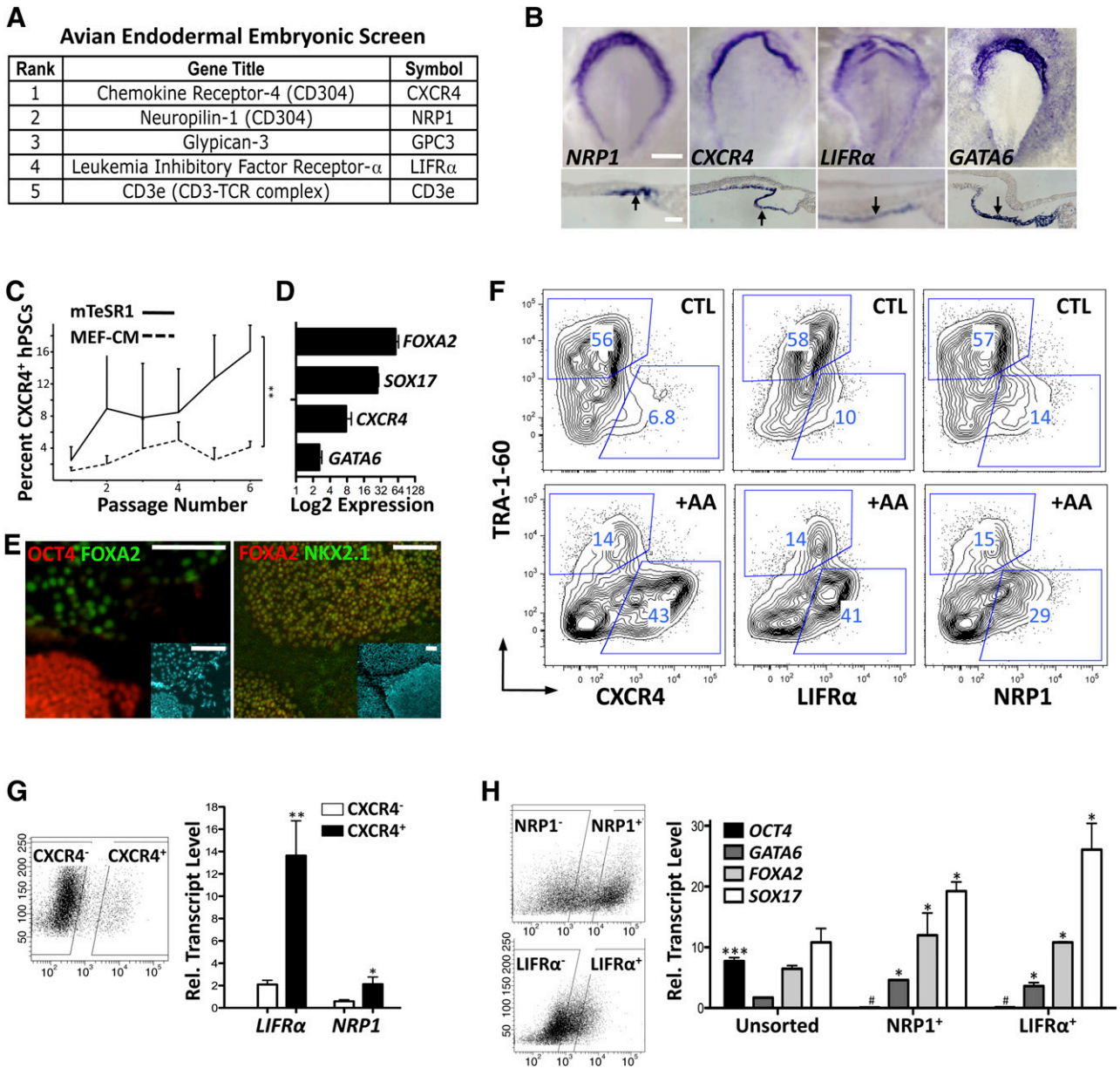

Figure 1. Evaluation of novel endoderm markers in the embryo and in human embryonic stem cells (hESCs); priming to definitive endoderm. **(A):** Cell surface receptors identified by an avian embryonic screen and tested in hESCs. **(B):** Expression analysis of *NRP1*, *CXCR4*, *LIFRα*, and control *GATA6* by whole-mount RNA in situ hybridization at stage HH4 in avian embryos. Transverse sections (lower panels) confirm staining to the lower endodermal cell layer (arrows). Scale bars = 500 μm (top panels) and 50 μm (bottom panels). **(C):** Emergence of stable CXCR4-positive population in hESCs in mTeSR1. Grouped flow cytometry values from CA2, H9, and iPS1.2 evaluated by analysis of variance (**, $p < .01$). **(D):** Summarized quantitative polymerase chain reaction data from CA2, H9, and iPS1.2 demonstrating increased endodermal marker expression in mTeSR1. **(E):** Immunofluorescence of primed H9 cells showing OCT4-positive colonies negative for regions of FOXA2-positive endoderm. FOXA2 expression overlaps with anterior foregut endoderm marker NKX2.1. Insets stained with 4′,6-diamidino-2-phenylindole show total cell numbers. Scale bars = 50 μm. **(F):** Flow cytometry analysis of CXCR4, LIFRα, and NRP1 versus TRA-1-60 in H9 cells adapted to mTeSR1 with and without 5-day treatment of 100 ng/ml AA. Endodermal markers expressed in basal conditions are augmented by AA, whereas TRA-1-60 is diminished. **(G):** Correlation of expression of *LIFRα* and *NRP1* with CXCR4-positive sorted CA2 cells (sorting gates shown on left). **(H):** Expression of pluripotency (*OCT4*) and endodermal markers in primed CA2 cells sorted for NRP1 and LIFRα (gating shown on left). Endodermal markers are higher in sorted populations, whereas *OCT4* expression is lower. Bar graphs show mean + SEM. *, $p < .05$; ***, $p < .001$; #, lower expression in sorted cells ($p < .01$); two-tailed Student's *t* test. Abbreviations: +AA, plus activin A; CTL, control; hPSCs, human pluripotent stem cells; MEF-CM, mouse embryonic fibroblast-conditioned medium.

the emergence of distinct morphological features such as focal densities appearing around 1 week (Fig. 2B). ALI culture also resulted in the formation of functional tight junctions, a hallmark of epithelialization, as documented by an increase in electrical potential (transepithelial electrical resistance) between apical and basal compartments (Fig. 2C) [33].

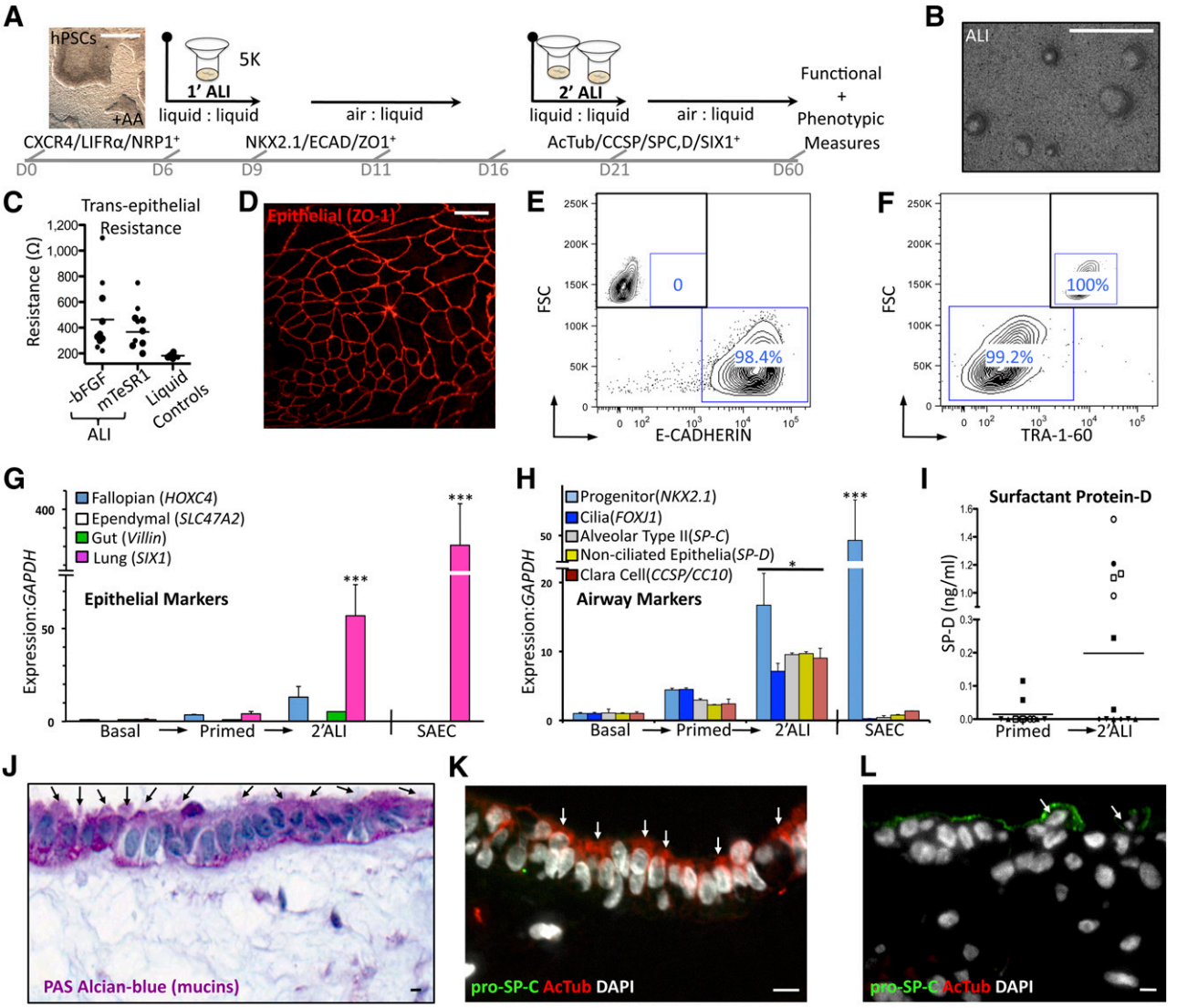

Figure 2. Differentiation of primed human embryonic stem cells (hESCs) to airway progenitors in vitro. **(A):** Optimized differentiation strategy demonstrating growth conditions enriching endodermal populations and ultimate airway cell formation. A hierarchical organization from hESCs to endodermal and definitive endoderm to airway progenitors emerges from this approach. Scale bar in microscopy image captured at ×2 is 500 μm. **(B):** Gross surface morphology of differentiated ALI cultures. Scale bar = 500 μm. **(C):** Transepithelial electrical resistance measurements of CA2, H9, and iPS1.2 grown in ALI. Control liquid-liquid cultures do not polarize. **(D):** Whole-mount en face staining for epithelial tight junction marker ZO-1 shows the presence of epithelial sheets on the surface of 2′ALI differentiated H9 cultures only. Scale bar = 10 μm. **(E,F):** Flow cytometric evaluation of epithelial (ECAD) and pluripotent (TRA-1-60) surface marker expression in 2′ALI in CA2. Insets show unstained controls. **(G):** Quantitative polymerase chain reaction-based expression screen of epithelial cell differentiation demonstrating robust increase of *SIX1* (lung associated) versus *Villin* (gut), *HOXC4* (fallopian), and *SLC47A2* (ependymal) in 2′ALI cultures from CA2 and H9 and control SAECs only. **(H):** Quantitative polymerase chain reaction-based expression screen of ciliation marker (*FOXJ1*) and secretory cell transcripts (*CCSP, SP-C, SP-D*) demonstrating a ∼10× upregulation in differentiated CA2 and H9 cultures only. In addition, 2′ALI differentiation results in upregulation of anterior foregut endodermal marker (*NKX2.1*) expression, which is also high in control SAECs. **(I):** SP-D enzyme-linked immunosorbent assay from apical supernatant. Conditioned media from liquid-liquid control hESC cultures or SAECs do not have detectable secreted SP-D. **(J):** PAS-Alcian blue staining (purple, mucins) shows a layer of ciliated cells (arrows) with underlying substratum. **(K, L):** Immunofluorescent costaining for acetylated tubulin (ciliation marker) and pro-SP-C (secretory cell marker). Colocalization of both markers is not observed, arrows indicate positive cells (hESCs). **(J–L):** Scale bars = 10 μm. Bar graphs show mean + SEM. Bars on scatter plots represent mean values. ∗, $p < .05$, ∗∗∗, $p < .001$; two-tailed Student's *t* test. Abbreviations: −bFGF, basic fibroblast growth factor-free; AcTub, acetylated tubulin; ALI, air-liquid interface; DAPI, 4′,6-diamidino-2-phenylindole; ECAD, E-cadherin; FSC, flow cytometry; GAPDH, glyceraldehyde-3-phosphate dehydrogenase; hPSCs, human pluripotent stem cells; PAS-Alcian blue, periodic acid-Schiff-Alcian blue; SAEC, small airway epithelial cell; SP-D, surfactant protein D.

Secondary ALI Results in Differentiation of Lung Epithelial and Secretory Cell Types

A secondary replating (2′ALI) permitted propagation of epithelialized E-cadherin and ZO-1 (TJP1)-positive, TRA-1-60-negative differentiated live cells (Figs. 2D–2F; supplemental online Fig. 2B, 2C). Because ZO-1 and ECAD (Fig. 2D, 2E) are general epithelial markers and are not specific to lung epithelium [34], we performed a differential expression screen using *SIX1* as a marker enriched in lung epithelium versus other ciliated epithelial markers from the fallopian tubes (*HOXC4*), brain (ependymal [*SLC47A2*]), and gut (*Villin*)

in order to distinguish the specific type of epithelia generated [35]. In addition to modest (fivefold) upregulation of the fallopian marker *HOXC4*, expression of the lung epithelial specific marker *SIX1* [36] was increased >50-fold by air-liquid differentiation in bFGF-free media (Fig. 2G), validating our hypothesis that priming hESCs in mTeSR1 with AA followed by ALI culture in bFGF-free differentiation media would enrich lung epithelial specification.

To further this characterization, we examined the expression dynamics for the anterior foregut progenitor marker *NKX2.1*, ciliated cell marker *FOXJ1*, and pulmonary secretory markers [37] *Secretoglobin 1A1/Clara Cell-Specific Protein* (*Uteroglobin/CCSP/CC10*) and *Surfactant Proteins C* and *D* (*SPC, SP-D*) under our differentiation scheme. Embryonic stem cells that underwent 2′ALI in bFGF-free differentiation media showed enhanced expression of not only progenitor marker *NKX2.1* but also ciliation (*FOXJ1*) and secretory markers *SP-C*, *SP-D*, and *CCSP*, alluding to the high level of complexity of the engineered lung tissue (Fig. 2H).

Subsequently, so as not to rely merely on transcript information to examine differentiation, protein measures were evaluated. Secreted SP-D is synthesized and secreted primarily by pulmonary epithelium [38] and was evaluated by enzyme-linked immunosorbent assay from washes of the apical (air-exposed) cells. Levels of secreted SP-D were found to be highest following 2′ALI culture, indicating that these conditions permitted progression from a progenitor to a more mature state (Fig. 2I). Next, to gain information about the single-cell level, histological examination was used to further characterize engineered lung tissue. Healthy airways secrete mucus to protect against infection and preserve moisture. Transverse sections of ALI cultures exhibited abundant mucus secretion, as demonstrated by strong periodic acid-Schiff-Alcian blue, which stains mucins a vibrant purple (Fig. 2J) [39]. In addition to their mucin coating, large areas of surface epithelium showed ciliation with this stain (Fig. 2J; supplemental online Fig. 2D). Further evidence of ciliation was seen by immunostaining using the ciliation-specific marker acetylated tubulin, expressed on the apical, or air-exposed, side of surface epithelium (Fig. 2K; supplemental online Fig. 3). Interestingly, distinct regions of cells positive for the type 2 alveolar epithelial cell-specific marker pro-SP-C were also abundant, but regions containing a mixture of both ciliated and secretory cells were not found by costaining (Fig. 2K, 2L). In summary, we have shown that hESC priming with mTeSR1 plus AA followed by 2′ALI culture leads to the generation of both ciliated and secretory airway epithelium in vitro.

Utility of hESC-Derived Airway Cells In Vivo Using a Lung Injury Model

In its progression from a progenitor to a mature state, airway epithelium acquires the ability to respond to pathogens to which it is presented when in contact with the external environment during respiration [40]. In order to functionally validate the lung epithelial cultures generated, the innate immune response of hESC-generated 2′ALI was challenged. Cultures were exposed to the proinflammatory bacterial endotoxin LPS, which elicited a significant increase in tumor necrosis factor α transcription in 2′ALI cultures grown in differentiation media only, whereas paired controls kept in hESC media had no effect (Fig. 3A). This finding indicates a lack of epithelial maturation in the control conditions despite the onset of epithelialization and polarization induced by ALI culture (Fig. 2).

Next, we quantified the number of input-to-output cells used in this study (Fig. 3B) to avoid merely reporting increased frequency (enrichment by attrition) of specific lineage-committed cells derived from hESCs by simply utilizing procedures that destroy cells incapable of endodermal differentiation, and thus survival, under these conditions. These analyses show that an overall increase of approximately 300-fold is obtained from a starting population of 1×10^6 mTeSR1-adapted hESCs primed for DE with high-dose AA to fully differentiated cells, thereby overcoming a major obstacle in the production of airway epithelia required for future applications and functional testing [5, 11].

Given this advance in obtaining high numbers of airway cells from hESCs, we developed a novel approach to examine hESC-derived airway cells in vivo using a murine recipient model of lung injury (Fig. 3C). We used intratracheal dilute HCl administration [21], adapting the system to immunodeficient mice capable of accepting human cells—an option not afforded to recent hESC-to-lung differentiation studies that were limited to in vitro drug assays because of generation of insufficient numbers of airway epithelial cells [10]. Dosage for chemical injury induction was determined by titrating tolerance of acid volume injected into the airways of NOD-SCID mice, where maximum penetration and survival was observed between 30–50 μl injected intratracheally, with perfusion robustly penetrating deeply into all lobes of the lung (supplemental online Fig. 4A). Similarly, cell delivery methods were tested using 15-μm fluorescent microspheres instilled intratracheally or injected intravenously 1 hour following injury. These experiments revealed an increased retention of beads delivered intravenous into the lung (supplemental online Fig. 4B). Transplanted cells were tested at high doses (2–2.5 $\times$ 10^5 cells) and low doses (0.5–1 $\times$ 10^5 cells) and assayed at different endpoints, revealing increased mortality at high doses of cells and thus establishing limits of cell doses for testing (supplemental online Fig. 4C). Histological examination of uninjured versus injured lung sections showed differences, with injured lungs displaying an increase in inflammatory cell infiltration (Fig. 3D) in addition to consistent reduction in SpO_2 used as a measure of lung physiological function, compared with uninjured mice (Fig. 3E).

Based on these results, we defined our model to utilize 30–50 μl of 0.1 N HCl instilled intratracheally to induce lung injury, followed by cellular transplantation intravenously 1 hour following injury. Using histology and SpO_2 as endpoints, the effects of several cell transplants were compared, including both control undifferentiated hESCs from liquid-liquid and air-liquid culture versus hESCs differentiated to airway cells (Fig. 2A, 3C). All cells were labeled with CM-DiI tracking dye (chemically modified to resist paraffin embedding) for in vivo detection of human cells in injured recipient NOD-SCID mice as well as human-specific Alu repeat DNA probe to define integrated cells.

hESC-Derived Airway Cells Aid in the Functional Recovery of the Lung Following Injury

Injured animals receiving hESC-derived lung epithelial cells (hESC-LECs) differentiated in 2′ALI showed integration of cells into the alveolar epithelium of the distal airways (Fig. 4A; supplemental online Fig. 4D, 4E). In contrast, recipients with injured lung tissue injected with undifferentiated hESCs had evidence of infiltrated cells into peripheral alveolar spaces and obstruction of airways (Fig. 4A). Differentiation of hESCs using ALI with embryonic stem media conditions failed to integrate in the appropriate regions of injured lung at early time points (1.5 weeks), similar to undifferentiated transplanted hESCs. Polymerase chain reaction for chromosome 17 α-satellite

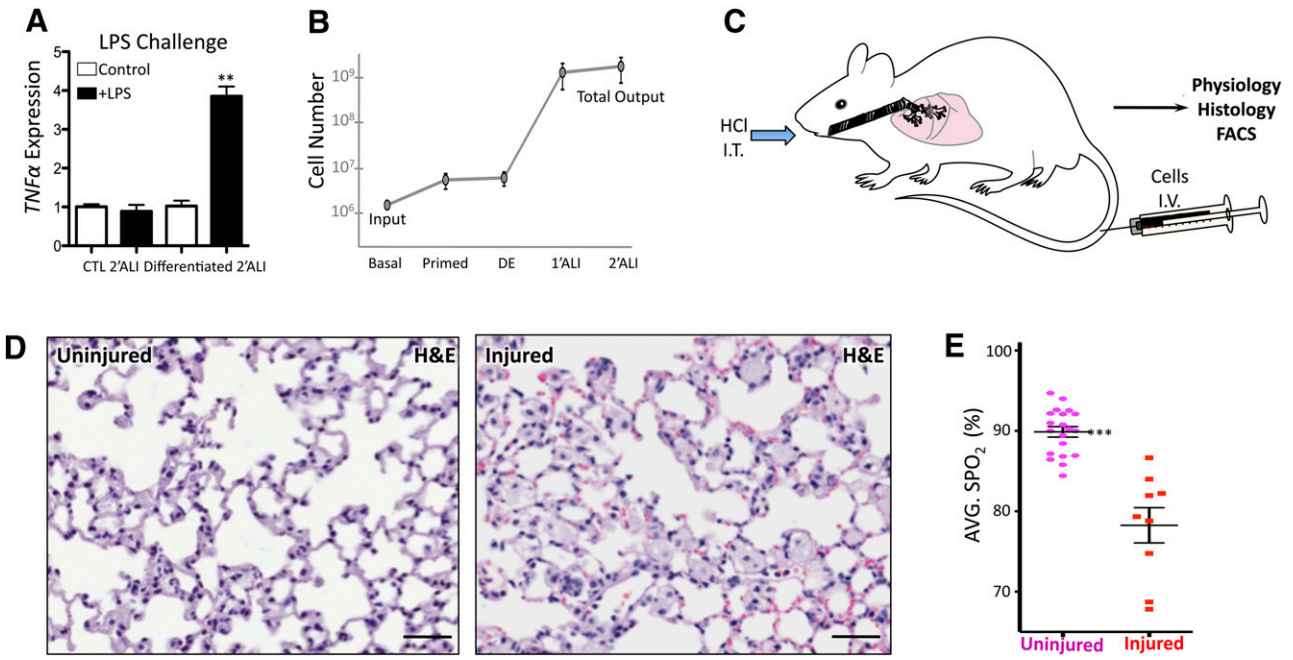

Figure 3. Functional differentiation and evaluation of an in vivo model. **(A):** LPS challenge of 2′ALI cultures. Primed human embryonic stem cells differentiated by 2′ALI show innate immune response by increasing *TNFα* expression in response to LPS. **(B):** Quantification of total cell numbers from initial basal cultures (mouse embryonic fibroblast-conditioned medium) to priming in mTeSR1 followed by addition of activin A (DE) and primary and 2′ALI cultures shows the increase in cell numbers obtained at each of these steps. **(C):** Animal model of lung injury using NOD-SCID mice. Intratracheal acid administration was followed by intravenous cell transplant. Efficacy of cell transplant beyond survival was evaluated by physiology, histology, and flow cytometry. **(D):** Representative histopathology of left lobe of control uninjured lung and lung following HCl-induced acute injury at 1.5 weeks showing evidence of inflammatory cell infiltration. Scale bars = 50 μm. **(E):** Oxygen saturation of control animals, taken as baseline versus animals receiving intratracheal HCl. ***, $p < .001$; two-tailed Student's *t* test. Abbreviations: ALI, air-liquid interface; CTL, control; DE, definitive endoderm; HCl, hydrochloric acid; H&E, hematoxylin and eosin; I.V., intravenously; I.T., intratracheally; LPS, lipopolysaccharide; AVG. SPO_2, average oxygen saturation; TNFα, tumor necrosis factor α.

gDNA revealed the presence of human DNA in lung homogenates up to 8 weeks following injection (Fig. 4B). Flow cytometry analysis was also performed at 8 weeks to verify retention levels thanks to CM-DiI labeling (supplemental online Fig. 4F), showing that chimerism of human cells was <1% (supplemental online Fig. 4G). Furthermore, mouse-specific CD11b staining was performed on harvested lungs in order to rule out CM-DiI uptake from cells phagocytosed by circulating mouse macrophages. Flow cytometry results demonstrated that CM-DiI-positive cells were found only in the CD11b-negative population (supplemental online Fig. 5).

Importantly, transplantation of hESC-derived lung epithelium enhanced the survival of airway-injured animals, whereas control mice transplanted with undifferentiated hESCs showed a marked reduction in survival by 1.5 weeks after injury (Fig. 4C). Concomitant with survival disparity, injured mice receiving hESC-derived lung epithelial progenitor cells (hESC-LEPs) showed recovery in SpO_2, whereas injured surviving mice transplanted with undifferentiated hESCs showed lowered SpO_2 levels (Fig. 4D). Furthermore, hESC-LEPs differentiated in 2′ALI in bFGF-free conditions demonstrated sustained survival and lung function based on SpO_2 for up to 6 weeks after transplantation, whereas long-term survival of injured mice transplanted with hESCs was minimal (Fig. 4E). On inspection of major organs at harvest, animals transplanted with hESC-LEPs examined at late time points had no observable tumors or teratoma formation.

With respect to the functionality of the integrated cells, CM-DiI-positive hESC-LEPs retained in the distal airways were found to costain with either CCSP or pro-SP-C, as detected by high-resolution confocal microscopy of lung sections (Fig. 4G). Furthermore, by gating acetylated tubulin-positive ciliated cells with flow cytometry, we were able to observe a significant number (~3%) of CM-DiI-positive cells within that fraction, indicating a contribution to the conducting airways (Fig. 4H). In aggregate, our results reveal that primed hESCs differentiated in dual 1′ALI and 2′ALI cultures in bFGF-free differentiation media give rise to functional airway cells (hESC-LEPs) that allowed tissue integration and that contribute to the physiological improvement of the lung.

Discussion

In this paper, we provide stepwise, hierarchical differentiation of hESCs to airway epithelial progenitor cells and subsequent functional pulmonary epithelial maturation that has not been reported to date (Fig. 5). Stepwise differentiation could be demarcated using multiplex phenotypic, morphological, and functional properties. These properties could be traced by illustrative heat mapping by progressive gain and loss of these markers throughout in vitro differentiation, resulting in progressive loss of pluripotency characteristics followed by transitional adaptation to DE, allowing eventual gain of mature lung epithelial properties including secretory protein expression, ciliation, and innate immune response. Novel endodermal markers identified using an avian embryonic screen, LIFRα and NRP1, aided in demarcating the early steps of directed hESC endodermal differentiation, although neither their use nor the use of CXCR4 provided an advantage in ameliorating ALI differentiation when sorted to pure populations.

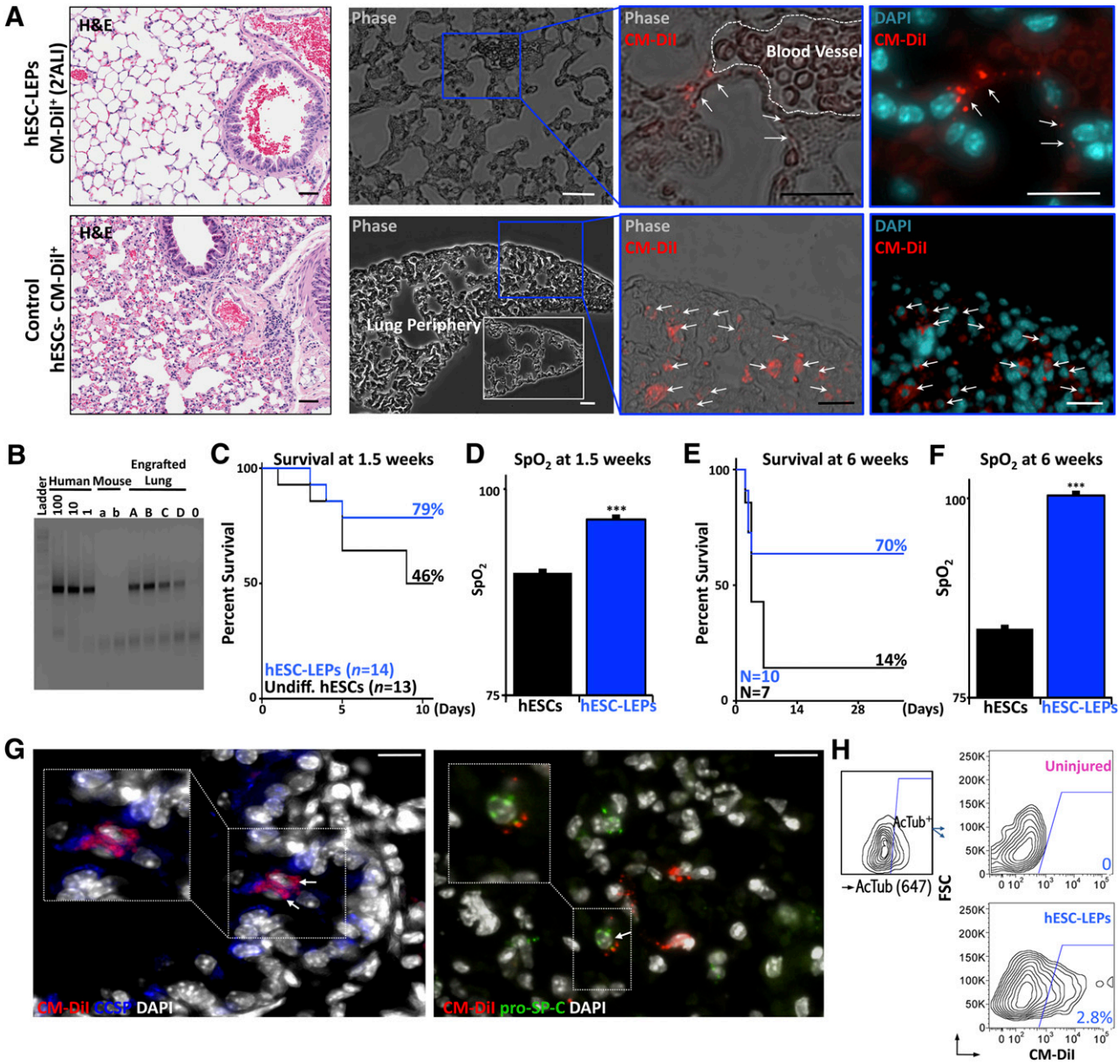

Figure 4. Cellular retention and physiological improvement in animals receiving hESC-derived LEPs (hESC-LEPs) following injury. **(A):** Far left: Histopathology of lungs from animals receiving either differentiated cells (top) or control hESCs (bottom) at 1.5 weeks after injury or transplantation. Note elevated cellular infiltration in animals receiving undifferentiated hESCs compared with differentiated cells (H&E stain). Subsequent panels: CM-DiI retention in lungs at 1.5 weeks. Top row: hESC-LEPs were observed in distal airways in close connection to vascular structures (pictured) but never within the vasculature. Reduced evidence of cellular infiltration and damage to alveolar architecture is seen as compared with controls. Bottom row: Control hESCs accumulated in the lung periphery and were not found to contribute to airway structures. White inset shows comparative peripheral lung morphology after hESC-LEP injection (CA2 shown). **(B):** Human-specific chromosome 17 polymerase chain reaction amplifying DNA from transplanted mouse lungs at 8 weeks after injury. Human standards are diluted at 100, 10, and 1 pg/μl. Input DNA content of unknowns is between 30–100 ng/μl. **(C):** Animals receiving control embryonic stem cells versus airway cells at 1.5 weeks demonstrated increased survival in treatment group. **(D):** SpO_2 is higher in animals receiving hESC-LEPs at 1.5 weeks. Survival **(E)** and SpO_2 **(F)** of the treatment group are also higher at 6 weeks. **(G):** Costaining of CM-DiI$^+$ integrated cells with either CCSP or pro-surfactant protein C. Representative confocal Z-stacks (10-μm depth) of lungs from transplanted mice 1.5 weeks after transplantation with airway cells. A subset of cells in regions retaining transplanted cells displays costaining of CM-DiI with either CCSP or pro-surfactant protein C, demonstrating functional differentiation in vivo (CA2 shown). **(H):** Flow cytometry examining CM-DiI$^+$ cell levels (PE channel) in acetylated-tubulin-positive ciliated cells (gating shown on left). CM-DiI$^+$ cells are observed in the acetylated tubulin-positive (ciliated cell) population in animals receiving acid injury and cellular transplantation (H9 shown). Bar graphs show mean + SEM. ***, $p < .001$; two-tailed Student's t test. Scale bars = 10 μm. Abbreviations: AcTub, acetylated tubulin; ALI, air-liquid interface; DAPI, 4′,6-diamidino-2-phenylindole; H&E, hematoxylin and eosin; hESCs, human embryonic stem cells; CM, conditioned medium; DiI+, CM-DiI-positive; FSC, flow cytometry; LEPs, lung epithelial progenitor cells; SpO_2, oxygen saturation.

Recently, advances made in the differentiation of hESCs to DE derivatives such as the lung have taken cues from developmental biology to carefully dissect growth factor-mediated progression of this lineage into foregut anterior endoderm and embryonic

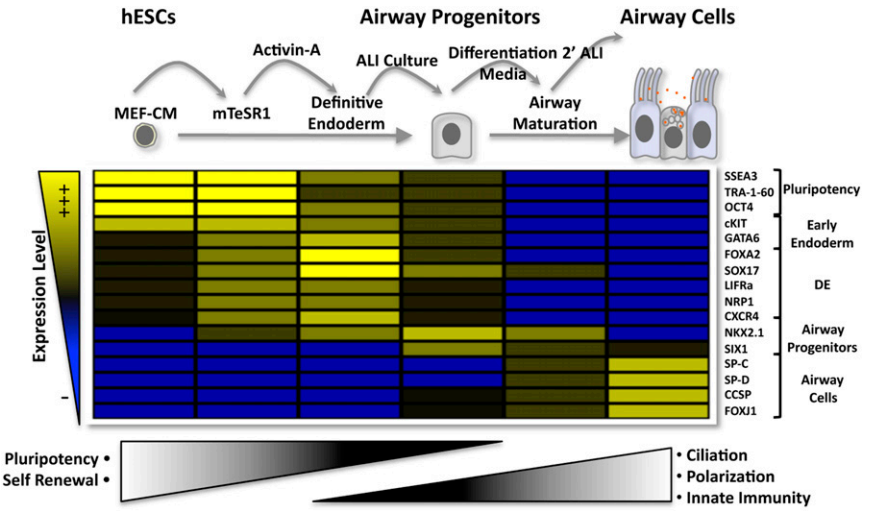

Figure 5. Illustrative heat map of the experimental approach used to guide cellular and molecular steps of hESC development to functionally mature airway cells in vitro. The hESCs are primed for endoderm by growth in chemically defined mTeSR1, where expression of newly defined LIFRα and NRP1 as well as CXCR4, GATA6, FOXA2, SOX17, and NKX2.1 is augmented. Expression of these markers is further increased by activin A treatment. Transfer to ALI culture results in epithelialization, and secondary passage removes dead cells and further augments the expression of terminal airway markers, leading to ultimate functional differentiation characteristics. Abbreviations: ALI, air-liquid interface; hESCs, human embryonic stem cells; MEF-CM, mouse embryonic fibroblast-conditioned medium; SP-C, surfactant protein C; SP-D, surfactant protein D.

lung stages [4, 6, 8, 10]. The complex growth factor combinations used in these studies have attempted to precisely recapitulate the environment encountered in the developing embryo. Despite documented precision, these studies failed to effectively calculate efficiencies of cellular yields or develop robust animal models to test differentiation capabilities in vivo [4, 6, 8, 10]. In contrast to these previous studies, our work takes an alternative approach to reports based on recapitulating mouse embryology and reveals four major, critical parameters for optimal generation of airway cells from hESCs: (a) preconditioning of cells in chemically defined media mTeSR1 plus AA that induces initial DE lineage priming; (b) growth of cells on Matrigel in feeder-free conditions to increase survival and maintenance of primed hESCs, as well as conditions conducive to translational applications [41]; (c) extension of the duration of differentiation via serial 1′ALI and 2′ALI cultures that increases survival and permits greater cellular yields required for future high-throughput drug screening and cell transplantation for lung regeneration in the human; and, importantly, (d) differentiation of cultures of secretory and ciliated epithelia, which is necessary for functional improvement in animal injury models.

Airway cells generated through initial DE formation followed by ALI are not homogenous but contain both secretory and ciliated epithelium. Previous studies have failed to show an in vivo benefit of using pure populations of transplanted cells in regenerative scenarios in the lung. We hypothesize that there is a lack of in vivo work using models to generate, for instance, pure populations of SP-C-positive type II alveolar epithelium produced from hESCs [42] because they are ineffective when used in isolation. Given the heterogeneous nature of the cells we generated in this study, we cannot rule out the possibility that nonlung cells present in 2′ALI cultures could have played a role in the recovery process following acid-induced lung injury. Future studies may try to compare the efficacy of hESC-LEPs versus other cellular sources currently being tested such as adult mesenchymal stem cells [43]. Such direct comparisons will ultimately prove whether pluripotent hESCs or more restricted adult multipotent sources are best to treat lung injury.

Conclusion

Collectively, we have shown the generation of functional human airway cells from hESCs. Differentiation of these cells to DE was informed by the use of two novel endoderm markers: LIFRα and NRP1. ALI culture and removal of bFGF resulted in epithelialization and the acquisition of functional characteristics including polarization, surfactant protein production, and innate immune response. The expansive nature of this differentiation protocol allowed us to test functional efficacy in an in vivo model of acute lung injury where, most important, these cells were able to persist in damaged areas of the lung and contribute to physiological recovery in vivo.

Acknowledgments

We thank Drs. Jon Draper and Carlos Pilquil for sharing valuable insight and antibodies; Hiroki Nagai for providing the *NRP1* in situ hybridization probe; Jelena Ulemek and Irene Tang for assistance with animal experiments; Steven Dingwall for providing teratoma and control mouse tissues; Lisa Laframboise for assistance with fluorescence in situ hybridization; Dr. Jennifer Sterns, from Dr. Michael Surette's laboratory in McMaster's Farncombe Family Digestive Health Research Institute, Hamilton, Ontario, Canada, for assistance in transepithelial electrical resistance analysis and making equipment available; Jamie McNicol for imaging analysis assistance; and Drs. Tony Collins and Eleftherios Sachlos for manuscript proofreading. This work was supported by a Canadian Institutes of Health Research (CIHR) Emerging Team Grant to M.B.

Author Contributions

B.A.S.M.: conception and design, collection and/or assembly of data, data analysis and interpretation, manuscript writing, final

approval of manuscript; C.A.: collection and/or assembly of data, data analysis and interpretation, manuscript writing, final approval of manuscript; R.M. and K.R.S.: collection and/or assembly of data, data analysis and interpretation, final approval of manuscript; J.B.L., A.F.-C., B.G., and Y.W.: collection and/or assembly of data, final approval of manuscript; G.S.: data analysis and interpretation, manuscript writing, final approval of manuscript; M.B.: conception and design, financial support, administrative support, collection and/or assembly of data, data analysis and interpretation, manuscript writing, final approval of manuscript.

Disclosure of Potential Conflicts of Interest

The authors indicate no potential conflicts of interest.

References

1 Zhang D, Jiang W, Liu M et al. Highly efficient differentiation of human ES cells and iPS cells into mature pancreatic insulin-producing cells. Cell Res 2009;19:429–438.

2 Cai J, Zhao Y, Liu Y et al. Directed differentiation of human embryonic stem cells into functional hepatic cells. Hepatology 2007;45:1229–1239.

3 Inami Y, Yoshikai T, Ito S et al. Differentiation of induced pluripotent stem cells to thymic epithelial cells by phenotype. Immunol Cell Biol 2011;89:314–321.

4 Mou H, Zhao R, Sherwood R et al. Generation of multipotent lung and airway progenitors from mouse ESCs and patient-specific cystic fibrosis iPSCs. Cell Stem Cell 2012;10:385–397.

5 Kadzik RS, Morrisey EE. Directing lung endoderm differentiation in pluripotent stem cells. Cell Stem Cell 2012;10:355–361.

6 Cheng X, Ying L, Lu L et al. Self-renewing endodermal progenitor lines generated from human pluripotent stem cells. Cell Stem Cell 2012;10:371–384.

7 Longmire TA, Ikonomou L, Hawkins F et al. Efficient derivation of purified lung and thyroid progenitors from embryonic stem cells. Cell Stem Cell 2012;10:398–411.

8 Green MD, Chen A, Nostro MC et al. Generation of anterior foregut endoderm from human embryonic and induced pluripotent stem cells. Nat Biotechnol 2011;29:267–272.

9 Van Haute L, De Block G, Liebaers I et al. Generation of lung epithelial-like tissue from human embryonic stem cells. Respir Res 2009;10:105.

10 Wong AP, Bear CE, Chin S et al. Directed differentiation of human pluripotent stem cells into mature airway epithelia expressing functional CFTR protein. Nat Biotechnol 2012;30:876–882.

11 Lung stem cells: Looking beyond the hype. Nat Med 2011;17:788–789.

12 Kroon E, Martinson LA, Kadoya K et al. Pancreatic endoderm derived from human embryonic stem cells generates glucose-responsive insulin-secreting cells in vivo. Nat Biotechnol 2008;26:443–452.

13 Kelly OG, Chan MY, Martinson LA et al. Cell-surface markers for the isolation of pancreatic cell types derived from human embryonic stem cells. Nat Biotechnol 2011;29:750–756.

14 Adewumi O, Aflatoonian B, Ahrlund-Richter L et al. Characterization of human embryonic stem cell lines by the International Stem Cell Initiative. Nat Biotechnol 2007;25:803–816.

15 Hong SH, Lee JH, Lee JB et al. ID1 and ID3 represent conserved negative regulators of human embryonic and induced pluripotent stem cell hematopoiesis. J Cell Sci 2011;124:1445–1452.

16 Alev C, Wu Y, Kasukawa T et al. Transcriptomic landscape of the primitive streak. Development 2010;137:2863–2874.

17 Hamburger V, Hamilton HL. A series of normal stages in the development of the chick embryo. 1951. Dev Dyn 1992;195:231–272.

18 Nakazawa F, Nagai H, Shin M et al. Negative regulation of primitive hematopoiesis by the FGF signaling pathway. Blood 2006;108:3335–3343.

19 Alev C, Nakano M, Wu Y et al. Manipulating the avian epiblast and epiblast-derived stem cells. Methods Mol Biol 2013;1074:151–173.

20 Kajstura J, Rota M, Hall SR et al. Evidence for human lung stem cells. N Engl J Med 2011;364:1795–1806.

21 Imai Y, Kuba K, Rao S et al. Angiotensin-converting enzyme 2 protects from severe acute lung failure. Nature 2005;436:112–116.

22 Luchtel DL, Boykin JC, Bernard SL et al. Histological methods to determine blood flow distribution with fluorescent microspheres. Biotech Histochem 1998;73:291–309.

23 Becker M, Nitsche A, Neumann C et al. Sensitive PCR method for the detection and real-time quantification of human cells in xenotransplantation systems. Br J Cancer 2002;87:1328–1335.

24 Risueño RM, Sachlos E, Lee JH et al. Inability of human induced pluripotent stem cell-hematopoietic derivatives to downregulate microRNAs in vivo reveals a block in xenograft hematopoietic regeneration. Stem Cells 2012;30:131–139.

25 Tada S, Era T, Furusawa C et al. Characterization of mesendoderm: A diverging point of the definitive endoderm and mesoderm in embryonic stem cell differentiation culture. Development 2005;132:4363–4374.

26 Trounson A. The production and directed differentiation of human embryonic stem cells. Endocr Rev 2006;27:208–219.

27 Yasunaga M, Tada S, Torikai-Nishikawa S et al. Induction and monitoring of definitive and visceral endoderm differentiation of mouse ES cells. Nat Biotechnol 2005;23:1542–1550.

28 D'Amour KA, Agulnick AD, Eliazer S et al. Efficient differentiation of human embryonic stem cells to definitive endoderm. Nat Biotechnol 2005;23:1534–1541.

29 Woodland HR, Zorn AM. The core endodermal gene network of vertebrates: Combining developmental precision with evolutionary flexibility. Bioessays 2008;30:757–765.

30 Hong SH, Rampalli S, Lee JB et al. Cell fate potential of human pluripotent stem cells is encoded by histone modifications. Cell Stem Cell 2011;9:24–36.

31 Ludwig TE, Levenstein ME, Jones JM et al. Derivation of human embryonic stem cells in defined conditions. Nat Biotechnol 2006;24:185–187.

32 Mizoguchi T, Verkade H, Heath JK et al. Sdf1/Cxcr4 signaling controls the dorsal migration of endodermal cells during zebrafish gastrulation. Development 2008;135:2521–2529.

33 Blume LF, Denker M, Gieseler F et al. Temperature corrected transepithelial electrical resistance (TEER) measurement to quantify rapid changes in paracellular permeability. Pharmazie 2010;65:19–24.

34 Tunggal JA, Helfrich I, Schmitz A et al. E-cadherin is essential for in vivo epidermal barrier function by regulating tight junctions. EMBO J 2005;24:1146–1156.

35 Ivliev AE, 't Hoen PA, van Roon-Mom WM et al. Exploring the transcriptome of ciliated cells using in silico dissection of human tissues. PLoS One 2012;7:e35618.

36 El-Hashash AH, Al Alam D, Turcatel G et al. Six1 transcription factor is critical for coordination of epithelial, mesenchymal and vascular morphogenesis in the mammalian lung. Dev Biol 2011;353:242–258.

37 Besnard V, Wert SE, Kaestner KH et al. Stage-specific regulation of respiratory epithelial cell differentiation by Foxa1. Am J Physiol Lung Cell Mol Physiol 2005;289:L750–L759.

38 Wong CJ, Akiyama J, Allen L et al. Localization and developmental expression of surfactant proteins D and A in the respiratory tract of the mouse. Pediatr Res 1996;39:930–937.

39 Dabbagh K, Takeyama K, Lee HM et al. IL-4 induces mucin gene expression and goblet cell metaplasia in vitro and in vivo. J Immunol 1999;162:6233–6237.

40 Martin TR, Frevert CW. Innate immunity in the lungs. Proc Am Thorac Soc 2005;2:403–411.

41 Wobus AM, Boheler KR. Embryonic stem cells: Prospects for developmental biology and cell therapy. Physiol Rev 2005;85:635–678.

42 Wang D, Haviland DL, Burns AR et al. A pure population of lung alveolar epithelial type II cells derived from human embryonic stem cells. Proc Natl Acad Sci USA 2007;104:4449–4454.

43 Lee JW, Fang X, Krasnodembskaya A et al. Concise review: Mesenchymal stem cells for acute lung injury: Role of paracrine soluble factors. Stem Cells 2011;29:913–919.

See www.StemCellsTM.com for supporting information available online.